Modelling the bubble size distribution in gas-liquid reactors with QMOM implemented with a new correction algorithm

Miriam Petitti

A. Nasuti, D.L.Marchisio, M.Vanni, G. Baldi, N. Mancini, F. Podenzani, A. Bennardo

Dept. Materials Science and Chemical Engineering, Politecnico di Torino (Italy)
ENI R&M, S.Donato Milanese (Italy)

miriam.petitti@polito.it

Outline

- Gas-liquid systems modeling: challenges and issues
- Simulation of a gas-liquid stirred tank (air-water):
  - Approach
  - Drag force evaluation
  - Population Balance Model
  - QMOM and correction algorithm
- Results:
  - Gas volume fraction
  - Bubble Size Distribution (BSD)
- Conclusion and possible next steps

Gas-liquid systems modeling: challenges and issues

- The simulation of poly-dispersed multiphase systems (i.e., constituted by droplets, particles and bubbles) is a complex problem
- Gas-liquid systems are the hardest to describe because fluid particles have no fixed shape or size:
  - Small bubbles à spherical
  - Medium bubbles à ellipsoidal
  - Big bubbles à spherical cup
- This has a tremendous impact on the interaction between the liquid (continuous phase) and the bubbles (disperse phase) for:
  - Momentum phase transfer
  - Mass phase transfer
  - Enthalpy phase transfer

Phase coupling

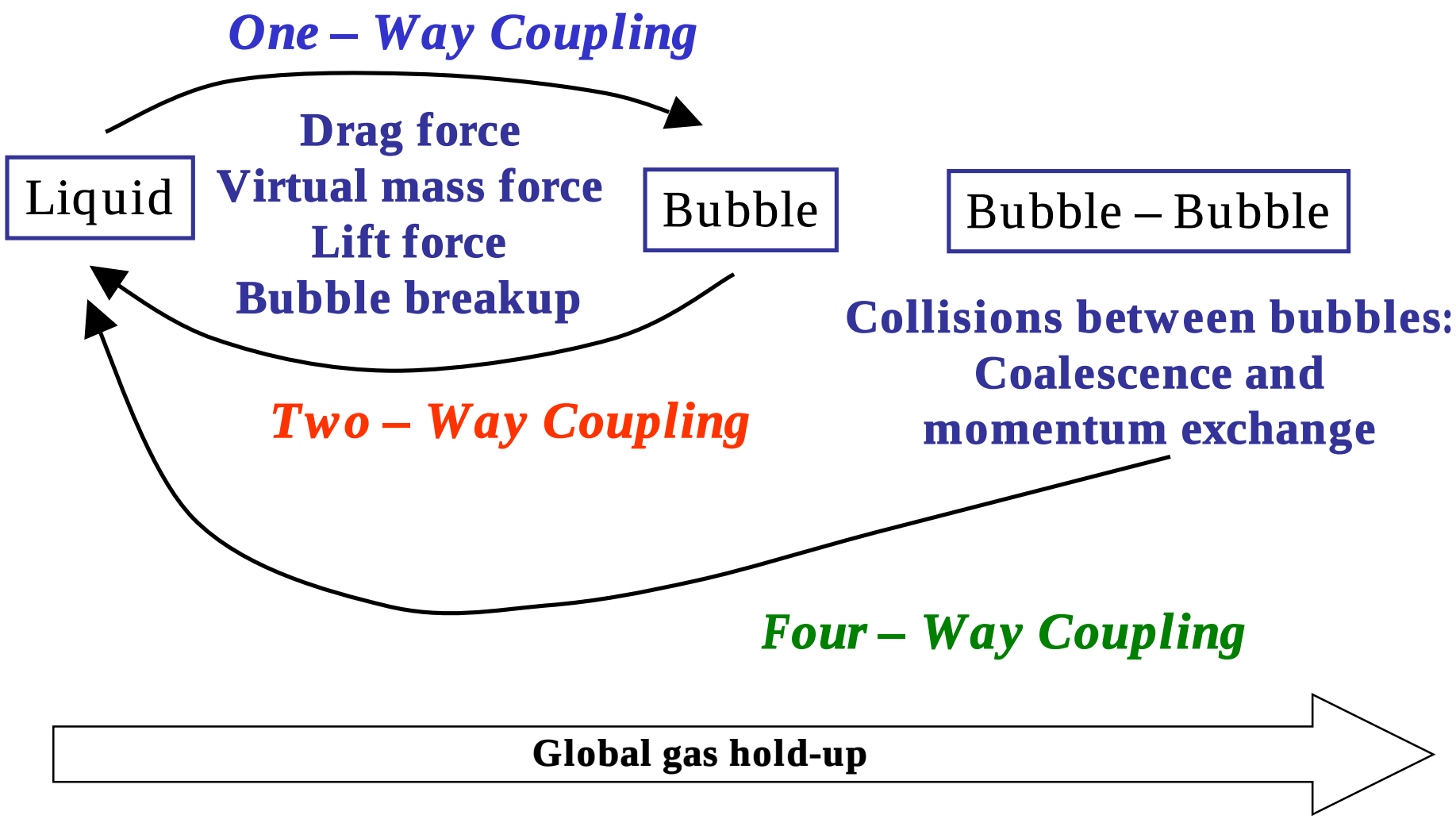

Approach: Four-way coupling

LIQUID-BUBBLE FORCES

- The fluid exerts a drag force on the bubbles that is related to the slip velocity, bubble size, turbulence intensity and bubble concentration (details in back-up slides)
- In addition there are the lift and virtual mass forces

BREAK-UP

The controlling mechanism is deformations induced by **turbulence**

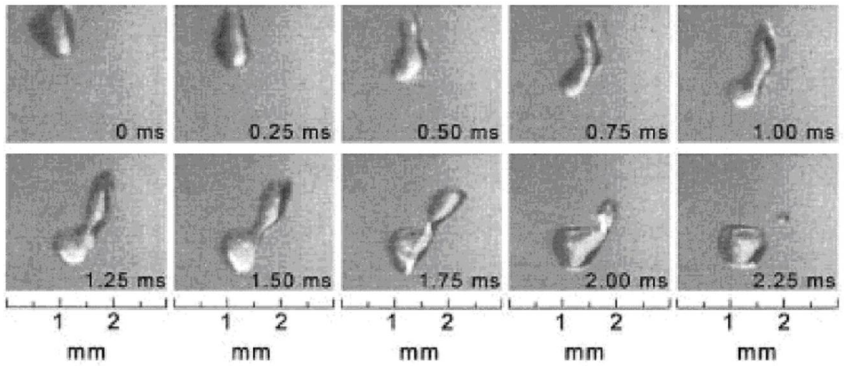

For gas bubbles **binary breakage** is the most common event

COALESCENCE

Three conceptual steps

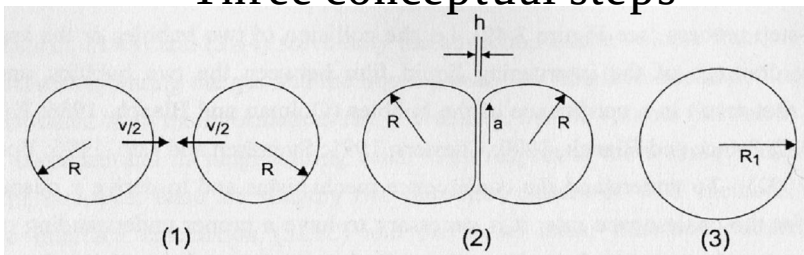

Bubbles come in close proximity because of turbulent eddies

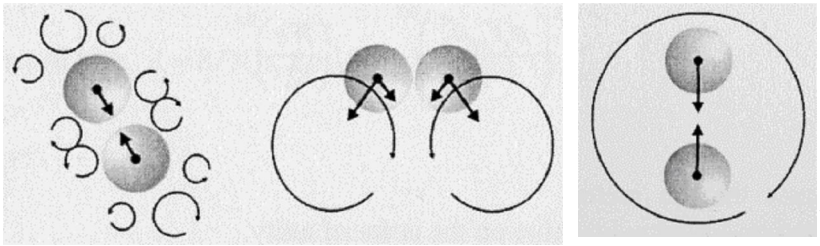

Approach

Eulerian Multifluid Model (Fluent)

- The phases are simulated as interpenetrating continua that obey transport equation and exchange momentum. Every phase has its own mass and momentum conservation equation.
- Phase interaction occurs via interfacial terms (especially drag). Closeness of the model used for this terms to the reality determines accuracy of the model.
- Most of the interfacial terms depend on particle size and most dispersed flows are not monodispersed, so knowledge of representative bubble diameter is essential.

Approach

- Expressions of the **drag term tailored specifically for bubbles** have been introduced as UDF
- A **solver for the population balance** equation has been included in the code to evaluate the bubble size distribution in every point of the system. The solver is based on the QMOM method, which allows accurate estimation of the integral properties of the BSD with moderate computational load (6 additional transport equations)
- **Proper expressions for bubble breakage and coalescence rates** have been tested and fitted to experimental data sets

Drag force evaluation

Usually in stirred reactors BSD is included in the range of ellipsoidal bubbles and is not so wide to cause a significant change in the bubble terminal velocity, according to Mendelsons's law.

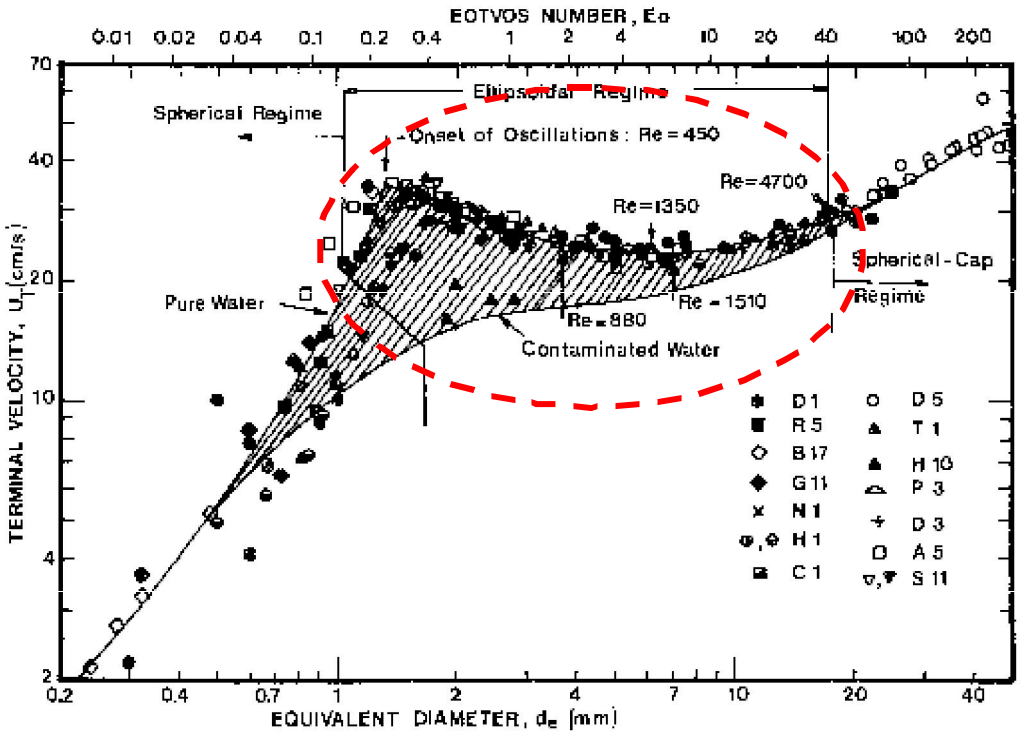

Drag force evaluation

The **drag coefficient** is evaluated from bubble terminal velocity: the **d_{32} of the local BSD** is considered and a **unique value for bubble terminal velocity** is used in the calculation.

$$C_D = \frac{4d_{32}\left(\rho_l - \rho_g\right)}{3\rho_l U_\infty^2}$$

The **damping effect of turbulence and the effect of high gas hold-up** are considered for the terminal velocity evaluation:

hold-up < 5%: about **13 cm/s** (turbulence)

hold-up > 5% :about **8.5 cm/s** (turbulence + effect near bubbles)

The **drag force** is evaluated on the basis of the local d_{32} and the local slip velocity between the continuous and dispersed phases.

Population Balance Equation

Its solution describes the evolution of bubbles size distribution:

Number
Density
Function

birth due to breakage

death due to breakage

$$\frac{\partial n(L_d,\overline{x},t)}{\partial t}+\nabla\cdot\left[\overline{U}_d\, n(L_d,\overline{x},t)\right]=\underbrace{\boxed{\int_{L_d}^{\infty} g(\lambda_d)\,b(L_d,\lambda_d)\,n(\lambda_d,\overline{x},t)\,d\lambda_d}}_{\mathbf{B_b}}-\underbrace{\boxed{g(L_d)\,n(L_d,\overline{x},t)}}_{\mathbf{D_b}}+$$

$$+\underbrace{\boxed{\frac{1}{2}\int_0^{L_d} h\left(\left(L_d^{\,3}-\lambda_d^{\,3}\right)^{1/3},\lambda_d\right)n\left(\left(L_d^{\,3}-\lambda_d^{\,3}\right)^{1/3},\overline{x},t\right)n(\lambda_d,\overline{x},t)\,d\lambda_d}}_{\mathbf{B_c}}-\underbrace{\boxed{n(L_d,\overline{x},t)\int_0^{\infty} h(L_d,\lambda_d)\,n(\lambda_d,\overline{x},t)\,d\lambda_d}}_{\mathbf{D_c}}$$

birth due to coalescence

death due to coalescence

Coalescence and breakup rates

Kernels (or frequencies) quantifies the rate with which bubbles COALESCENCE and BREAK.
Several expressions are available in the literature but in this work the following have been used (Laakkonen et al., 2006):

BREAKUP KERNEL

$$g(L_d) = C_1 \varepsilon^{1/3} \operatorname{erfc}\left(\sqrt{C_2 \frac{\sigma}{\rho_c \varepsilon^{2/3} L_d^{5/3}} + C_3 \frac{\mu_c}{\sqrt{\rho_c \rho_d} \varepsilon^{1/3} L_d^{4/3}}} \right)$$

Binary breakage, C_1 from fitting

COALESCENCE KERNEL

$$h(\lambda_d, L_d) = C_7 \varepsilon^{1/3} (\lambda_d + L_d)^2 \left(\lambda_d^{2/3} + L_d^{2/3}\right)^{1/2} \eta(\lambda_d, L_d)$$

C_7 = 0.88
(from theory)

$$\eta(\lambda_d, L_d) = \exp\left(-C_8 \frac{\mu_c \rho_c \varepsilon}{\sigma^2} \left(\frac{\lambda_d L_d}{\lambda_d + L_d} \right)^4 \right)$$

Quadrature Method of Moments

The PBE is solved in terms of the first $k = 2N$ **moments** of the Number Density Function (NDF) $n(L)$:

$$\frac{\partial}{\partial t}\left(\overline{\rho}_d m_k\right) + \nabla\left(\rho_d \hat{u}_d^k m_k\right) = \overline{\rho}_d S_k \qquad k = 0,1,2,3,4,5$$

where the moments m_k refer to bubble size L: $\longrightarrow$ $m_k \equiv \int_0^{+\infty} n(L) L^k dL$

The **closure** on the moments source terms S_k, concerning bubble coalescence and breakup, is obtained by resorting to a **quadrature approximation** :

$$\int_0^{+\infty} n(L) f(L) dL \approx \sum_{i=1}^{N} w_i f(L_i)$$

weights nodes

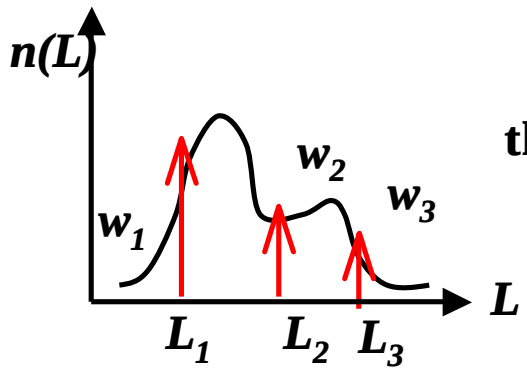

***N* = 3**

the first 6 moments are tracked

$$S_k = \frac{dm_k}{dt} = \underbrace{\sum_{i=1}^{N_d} g(L_i) w_i \overline{b}_i^{(k)}}_{B_{bk}} - \underbrace{\sum_{i=1}^{N_d} L_i^k g(L_i) w_i}_{D_{bk}} + \underbrace{\frac{1}{2}\sum_{i=1}^{N_d} w_i \sum_{j=1}^{N_d} w_j \left(L_i^3 + L_j^3\right)^{k/3} h(L_i, L_j)}_{B_{ck}} - \underbrace{\sum_{i=1}^{N_d} L_i^k w_i \sum_{j=1}^{N_d} h(L_i, L_j) w_j}_{D_{ck}}$$

QMOM and Moments corruption

The population balance is coupled with the multi-fluid model through the moment transport equations. The moments can be considered as **scalars** that are convected, mixed and diffused. However they are linked by **mathematical relationships** that assure the physical existence of the underlying distribution.

The independent transport of the moments does not preserve these relationships, that are **altered** by the discretization schemes used by the CFD code, and can therefore create a **set of corrupted (and not valid) moments**.

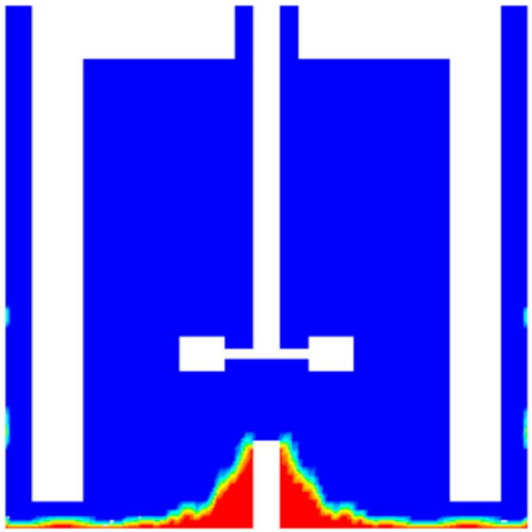

Non - valid moment set

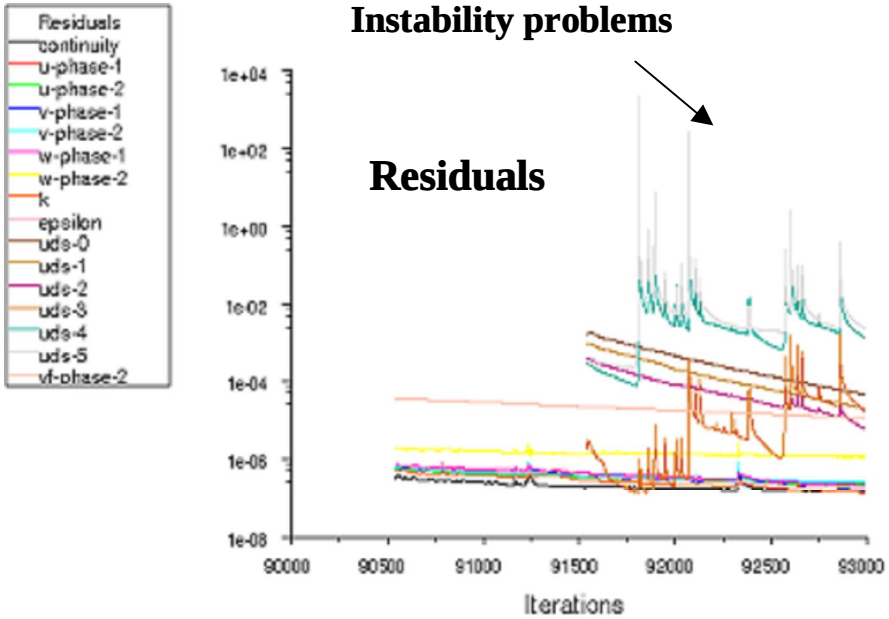

Negative moments, relationships altered

QMOM and Moments validity test

The **validity of the moment set is checked** by asserting the **positivity** of the **determinants** of Hankel-Hadamard (Shohat e Tamarkin, 1943):

$$\Delta_{n,l} = \begin{vmatrix} m_n & m_{n+1} & \dots & m_{n+l} \\ m_{n+1} & m_{n+2} & \dots & m_{n+l+1} \\ \vdots & \vdots & \vdots & \vdots \\ m_{n+l} & m_{n+l+1} & \dots & m_{n+2l} \end{vmatrix} \geq 0 \qquad \text{for } n = 0,1 \text{ and } l \geq 0$$

These conditions **for the first few moments** $\{m_0, m_1, m_2, m_3\}$ are equivalent to the **convexity check** of the curve $\ln(m_k)$ in function of k:

$$m_k m_{k-2} - m_{k-1}^2 \geq 0$$

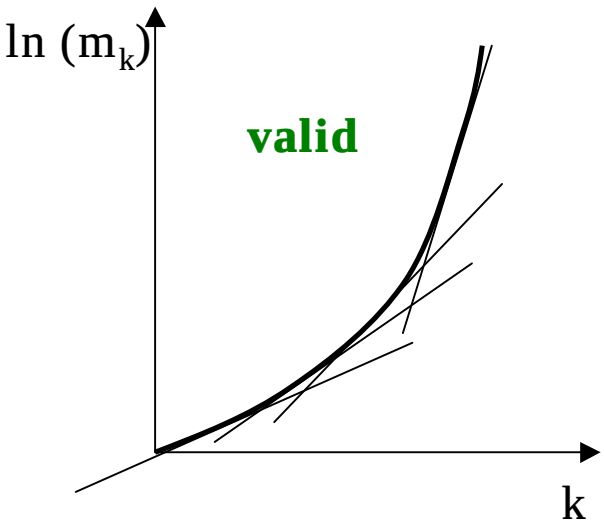

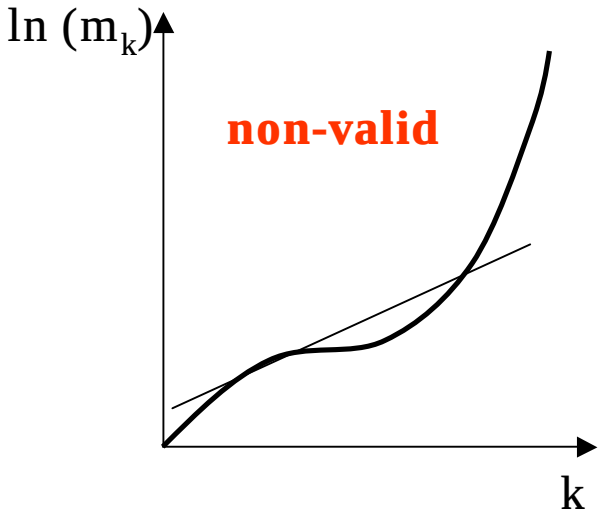

QMOM and Moments correction

Minimum Square Gradient Algorithm

(McGraw 2006)

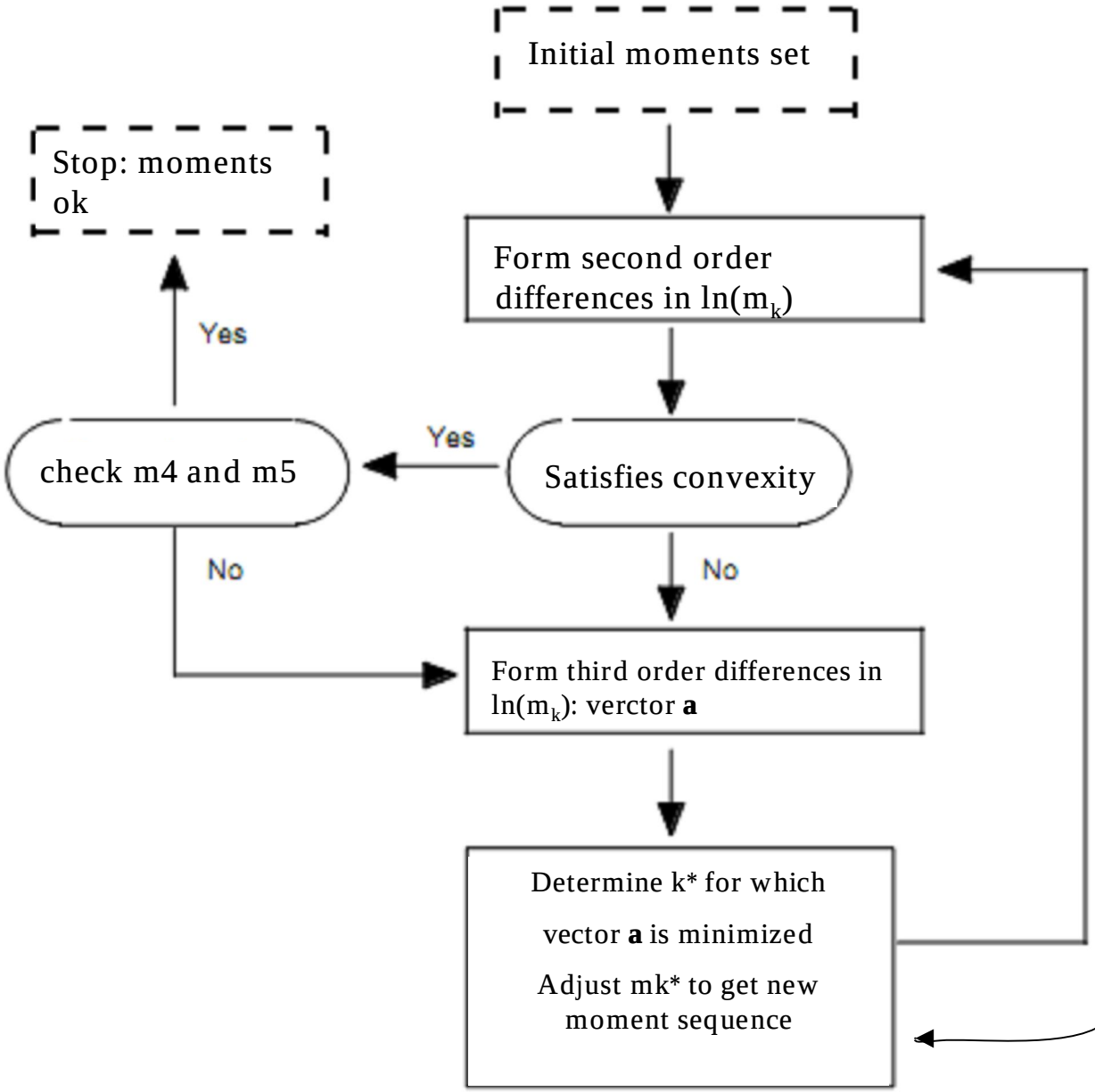

Adjust that moment which after adjustment maximizes smoothness through minimization of a vector related to third order differences

QMOM and Moments correction

1) **In certain cases** the iterative algorithm enters an **infinite loop** and does not manage to correct the moment sequence.

In these cases the **moment set is re-built through two log-normal distributions** whose parameters are obtained **from the first 4 moments** of the original set that must be corrected **(Wright 2007)**

NDF: $$n_L(L) = N_T \cdot \frac{\exp\left[\frac{-(\ln L - \mu)^2}{2\sigma^2}\right]}{L\sigma\sqrt{2\pi}}$$

moments: $$m_k = N_T \exp\left(k\mu + \frac{k^2\sigma^2}{2}\right)$$

NDF(1) from m_0, m_2, m_3 **NDF(2)** from m_0, m_1, m_3

Moments evaluated as averages of the moments of the two distributions

2) **Control on gas volume fraction, particularly useful at higher gassing rates:** **if gas vof < 10^{-3} ⟶ sources = 0; m_k = 0; d_{32} = db_{inlet}**

Without this change at higher gassing rates it is observed the formation of zones with $m_5 < 0$, tending to spread in neighbouring zones

Effects of moments correction

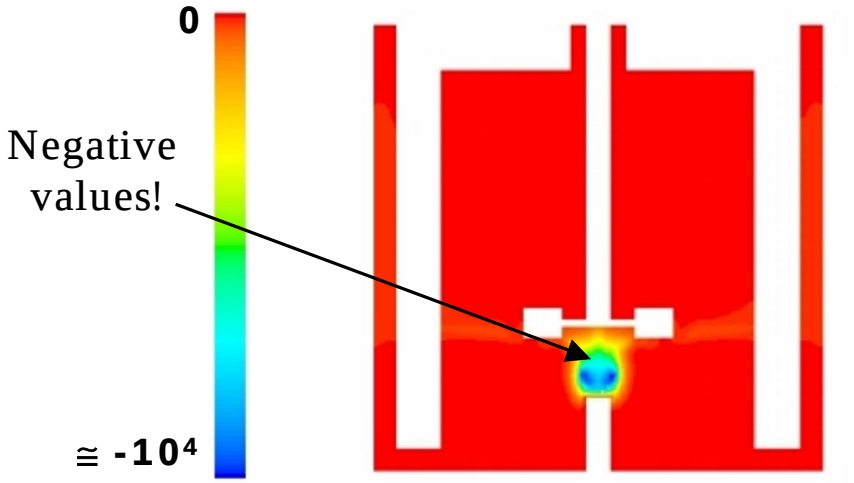

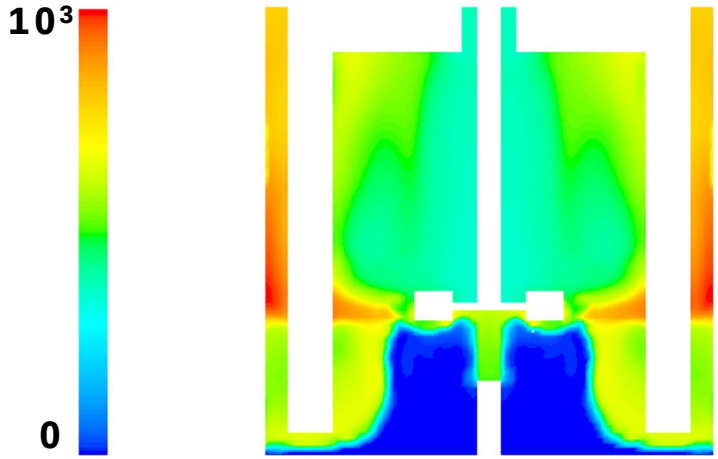

m_2 without correction

m_2 with correction

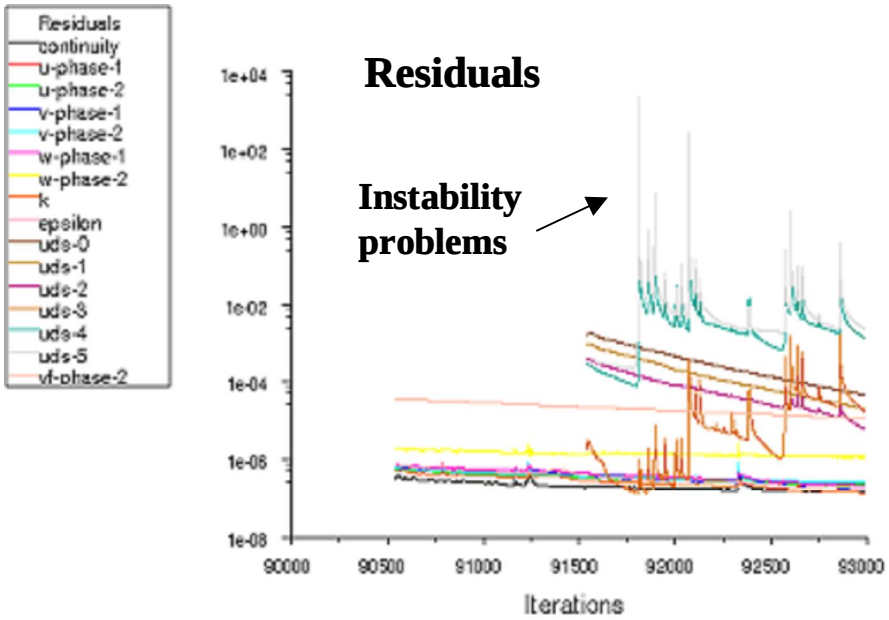

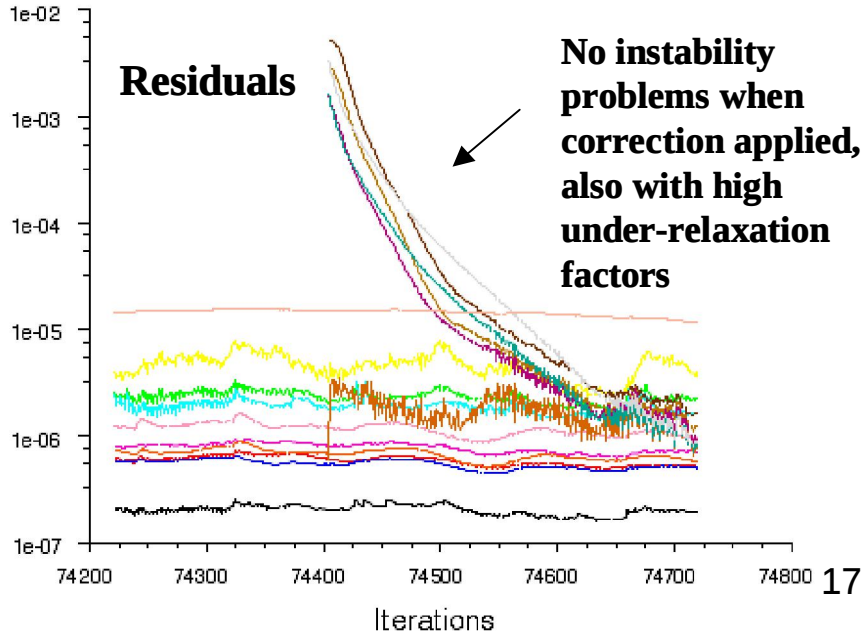

Effects of moments correction

"Lucky" simulation with low numerical diffusion for the moments

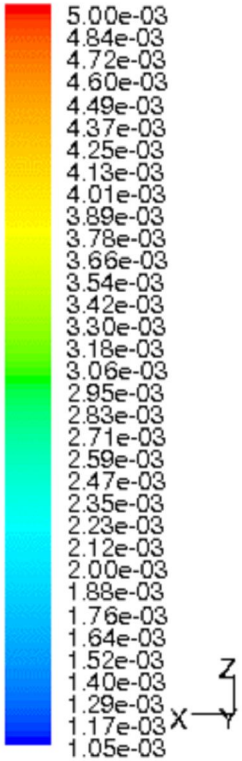

d_{32}

without correction

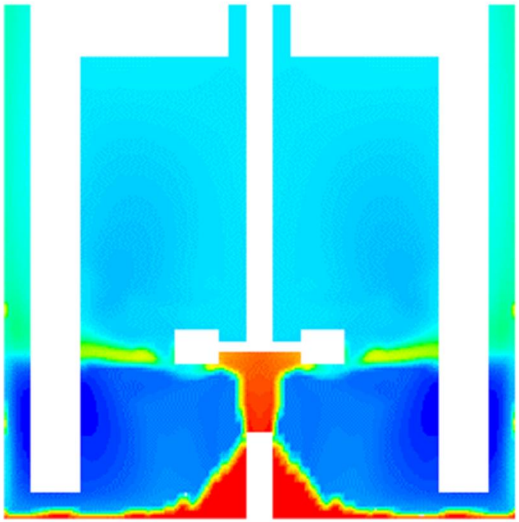

d_{32}

with correction

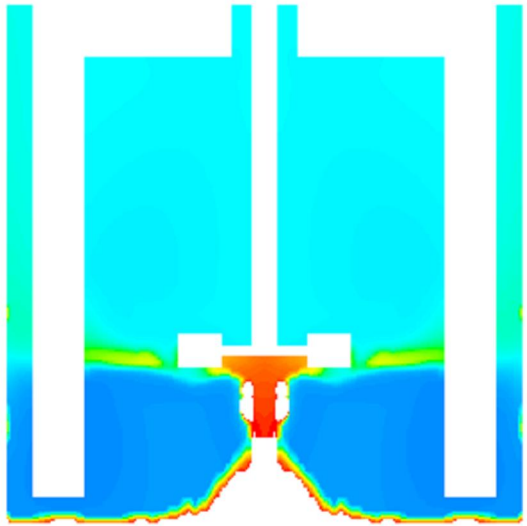

The correction algorithm does not alter the physical behaviour of the system, the bubble size distribution

Reactor configuration - 1

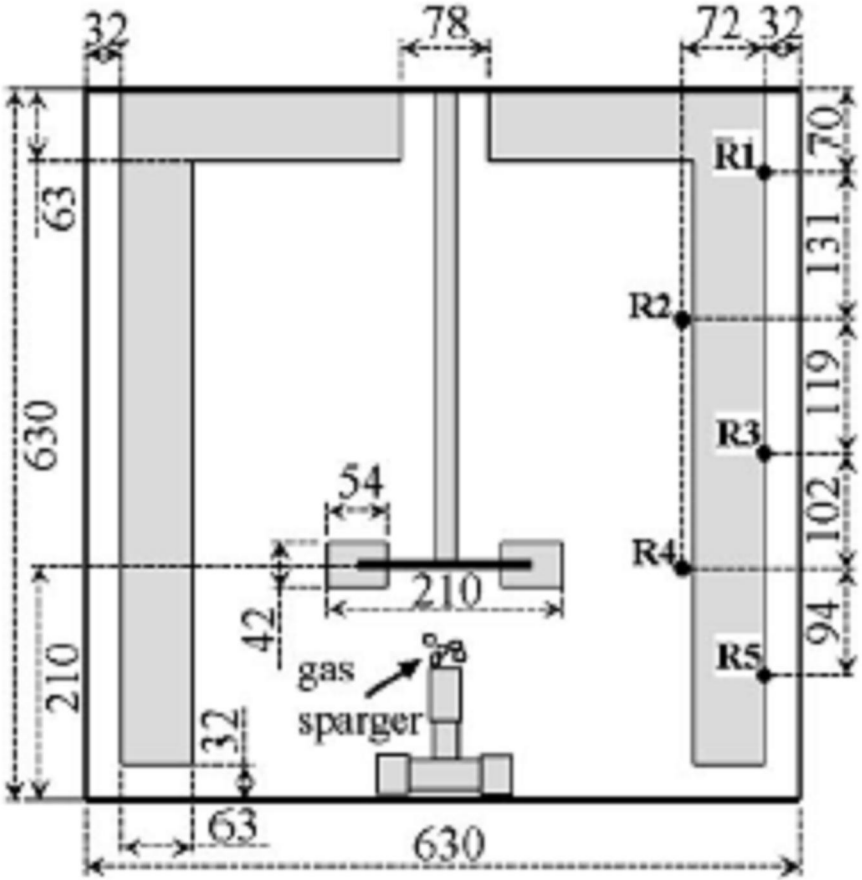

Porous sparger

Standard Rushton turbine
Baffles and blades width: 1.03 cm
Shaft diameter: 3.3 cm
Disk diameter: 13.6 cm
Turbine diameter: 21cm
Disk width: 1.06 cm
Sparger position: z = -10.5 cm; d = 3.3 cm
Sparger width d = 15 mm

Reactor volume: 194 liter

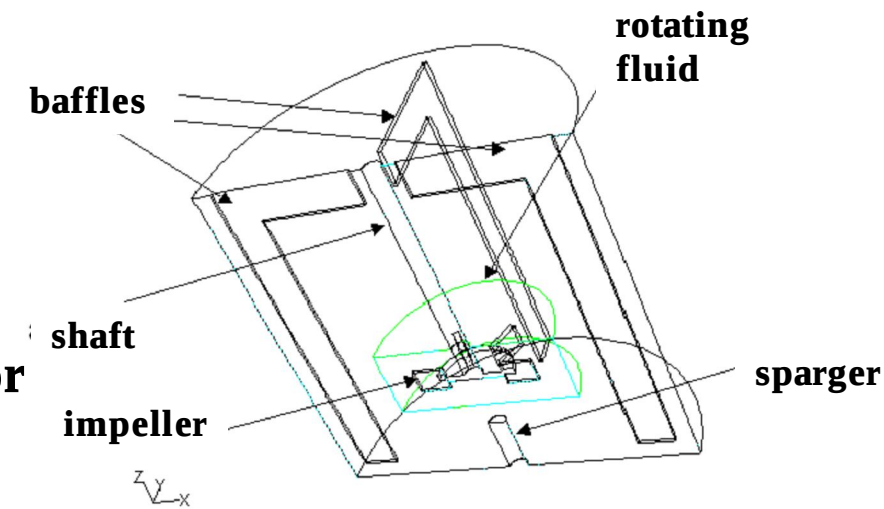

Computational domain on half reactor

à N_{cells}: 226776

Reactor configuration - 2

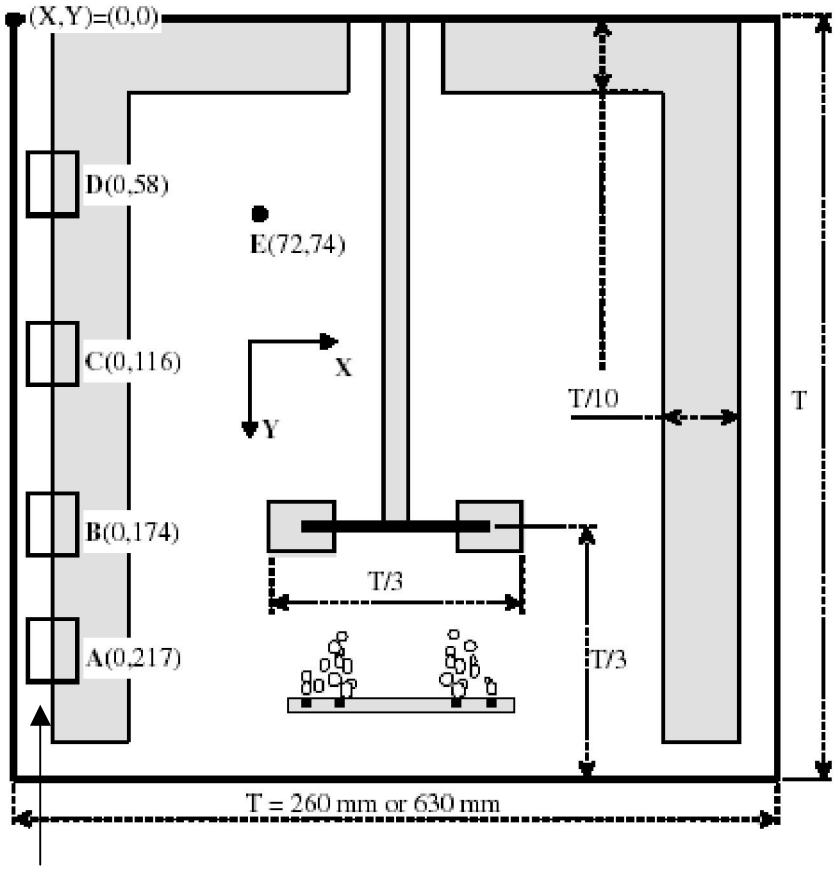

Ring sparger (12 holes 2 mm of diameter)

Standard Rushton turbine

Baffles and blades width: 1.03 cm

Shaft diameter: 3.3 cm

Disk diameter: 13.6 cm

Turbine diameter: 21cm

Disk width: 1.06 cm

Sparger position: z = -10.5 cm; d = 3.3 cm

Sparger width d = 15 mm

Reactor volume: 194 liter

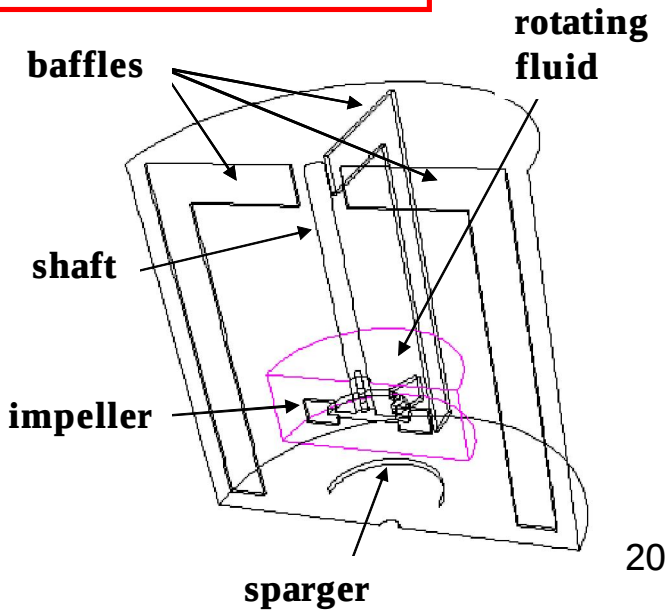

Computational domain on half reactor

à N_{cells}: 226776

Results-fluid dynamics

The fluid dynamics predicted by the model was also tested for a standard geometry stirred reactor of 15.4 liter, agitated by a Rushton turbine, in terms of:

-Velocity profiles

-Fluid dynamics regime transitions

-Gas cavity structure transitions

- Power dissipated

The agreement with experimental data and/or empirical correlations is good

Results – gas distribution

GAS VOLUME FRACTION

Reactor
configuration 1

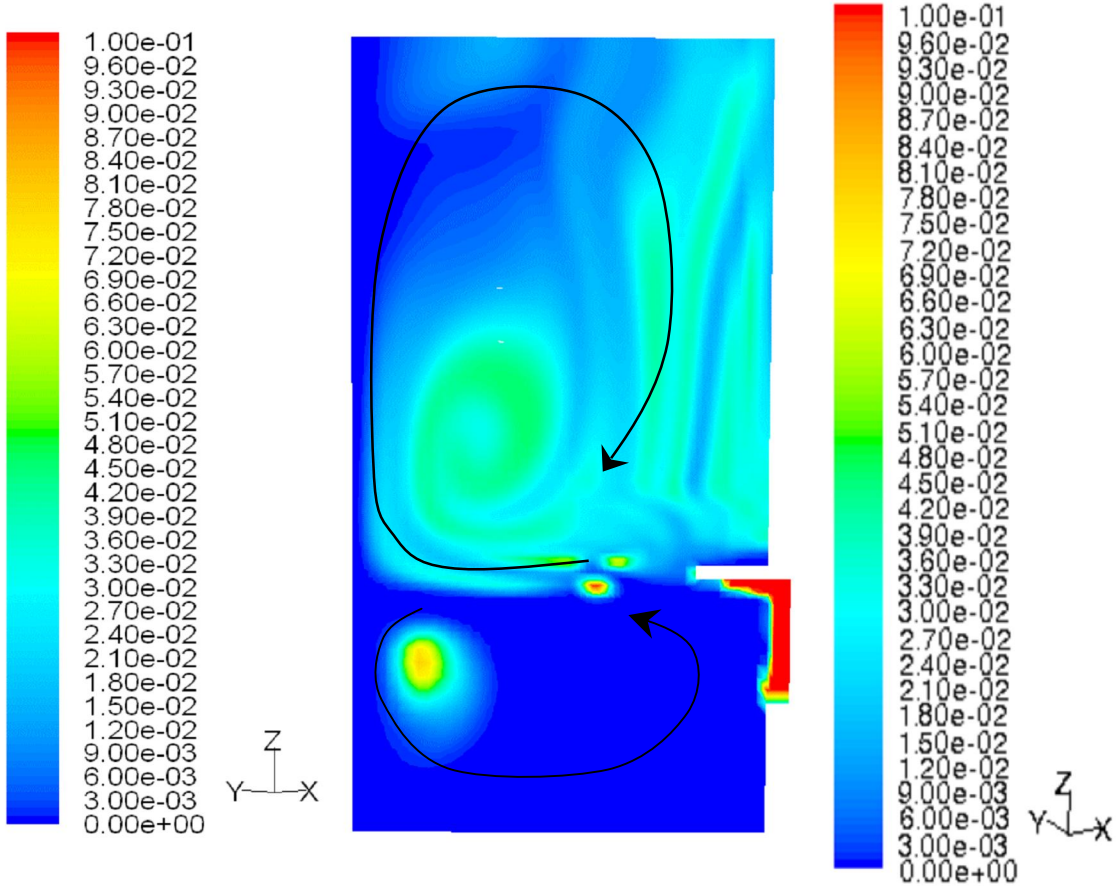

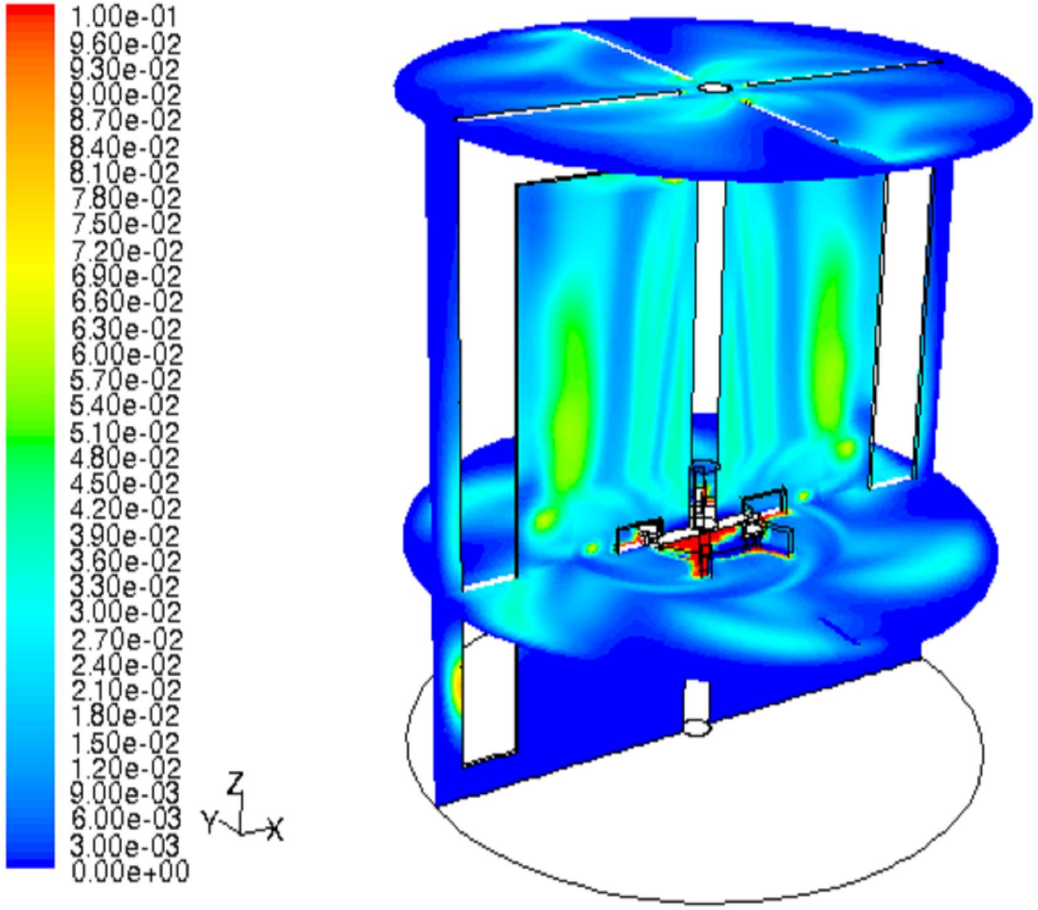

Results – Gas hold-up

Reactor configuration 2 N = 390 rpm

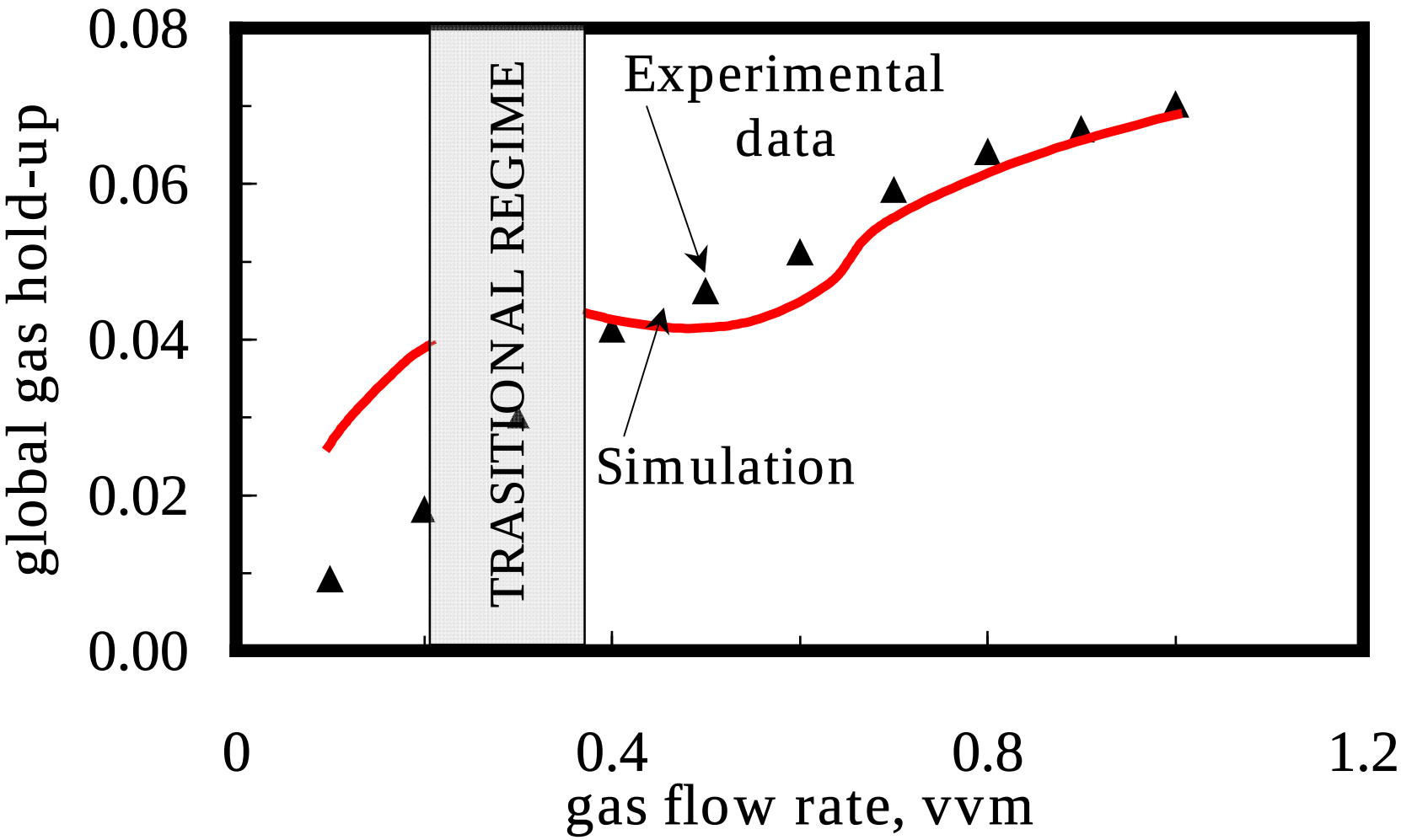

Results Bubble size distribution

8 different operating conditions for reactor configuration 1 and 7 different conditions for reactor configuration 2 were considered resulting in the following best fit values:

C_1= 6 (from fitting) and C_7 =0.88 (from theory)

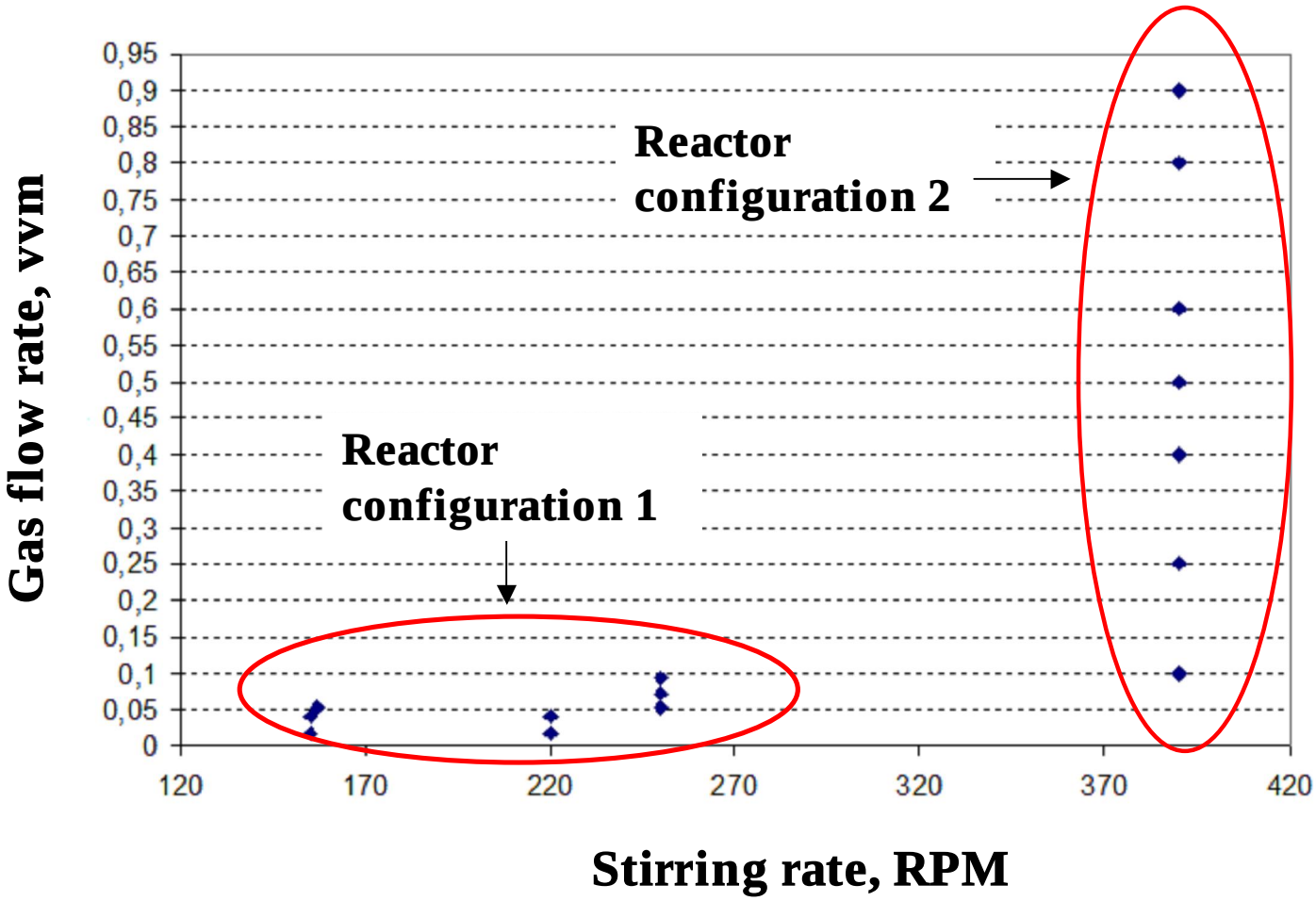

Results – Bubble size distribution

Reactor configuration 1

***N* = 250 RPM; 0.093 vvm**

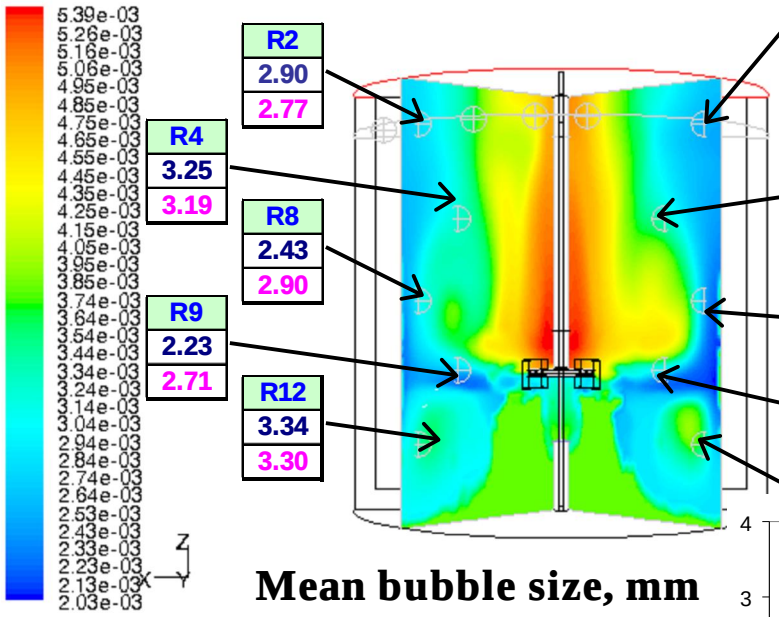

Mean bubble size, mm

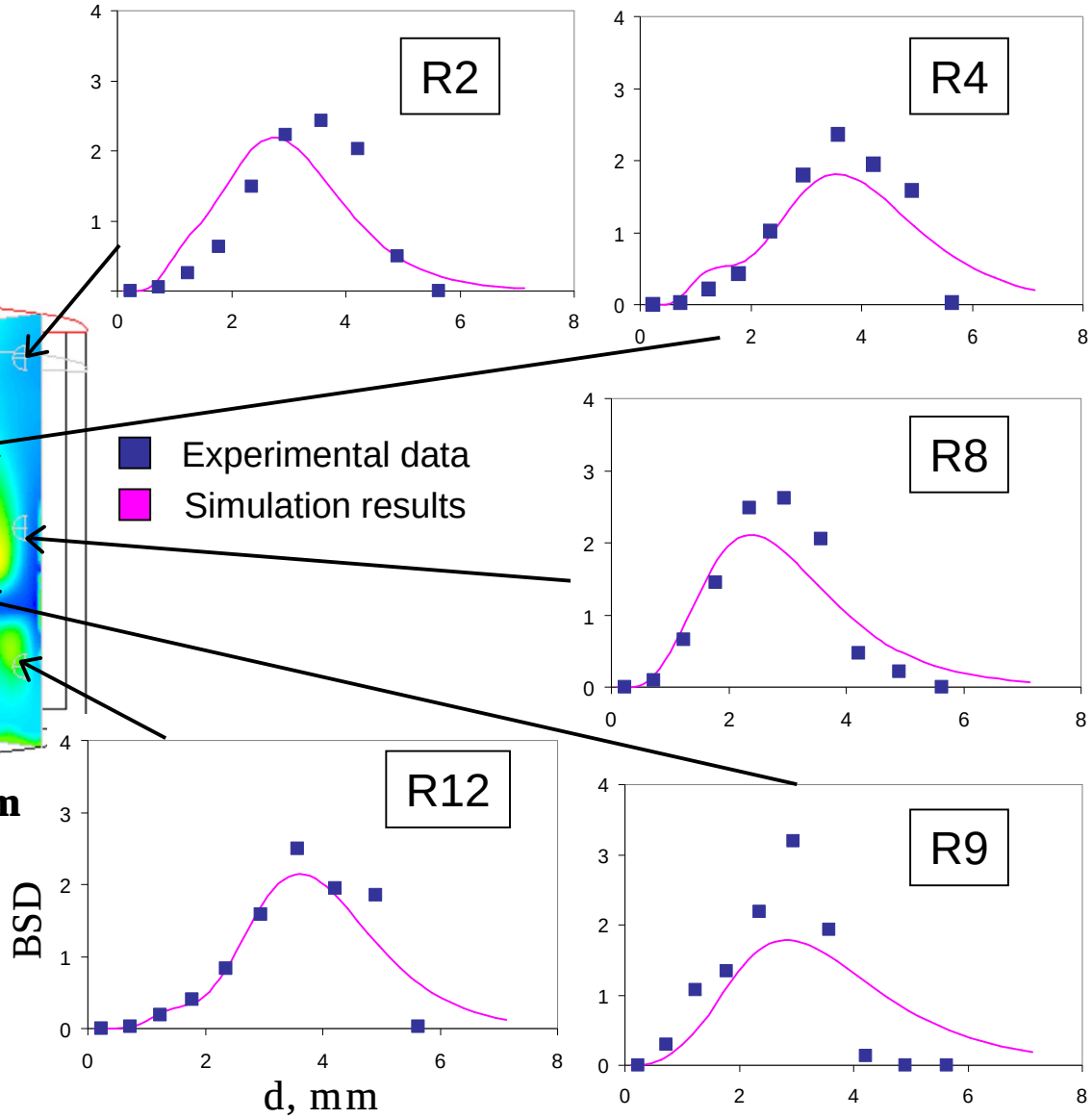

Results – Bubble size distribution

Reactor configuration 1 – *N* = 250 RPM; 0.093 vvm

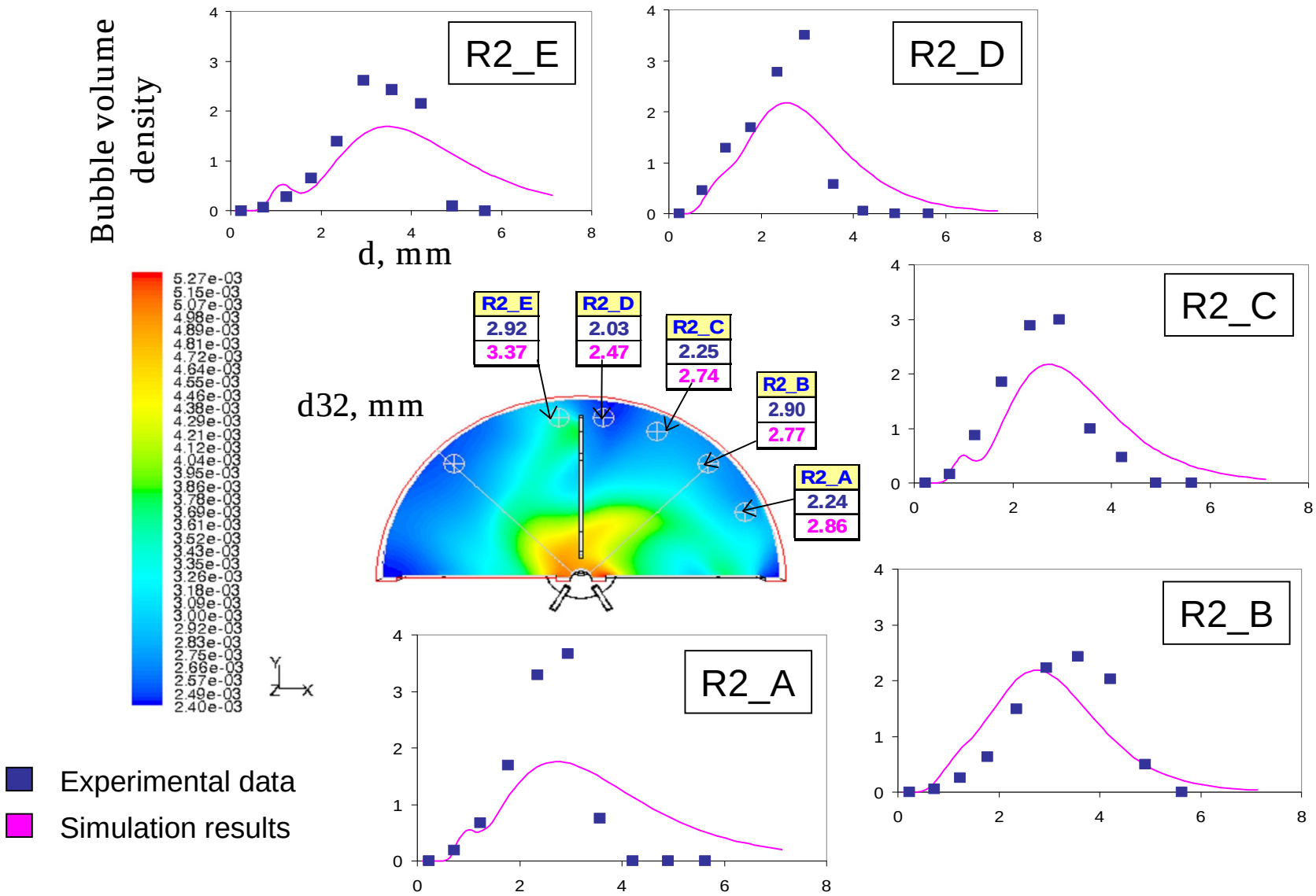

Results – Bubble size distribution

Reactor configuration 1

N **= 157 RPM; 0.052 vvm**

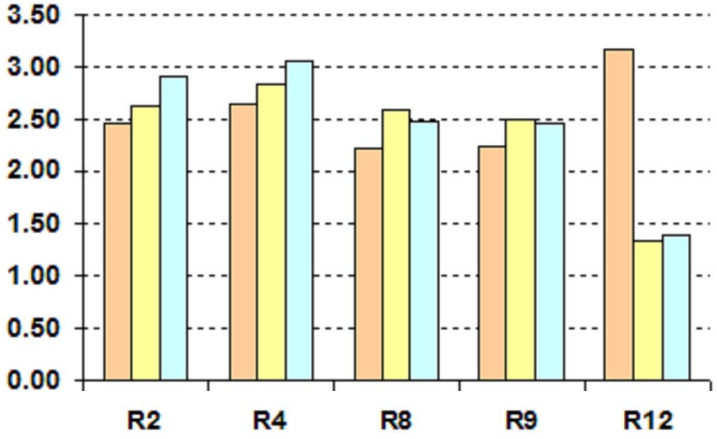

N **= 250 RPM; 0.052 vvm**

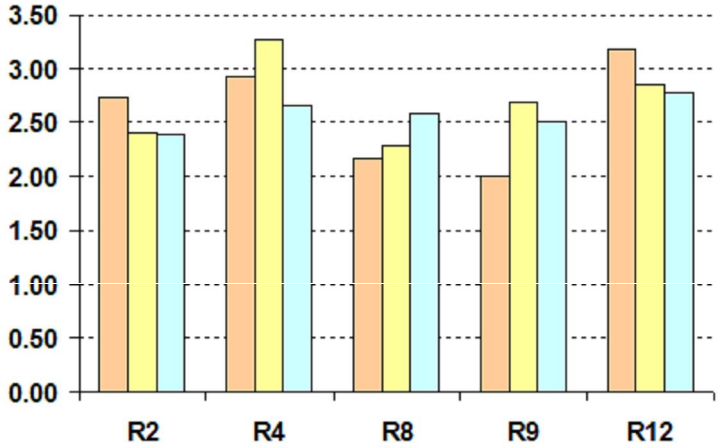

N **= 250 RPM; 0.072 vvm**

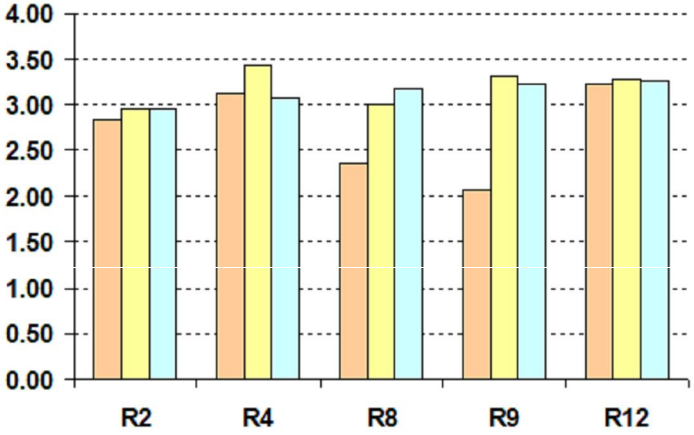

Experimental

Simulation (45°)

Simulation (135°)

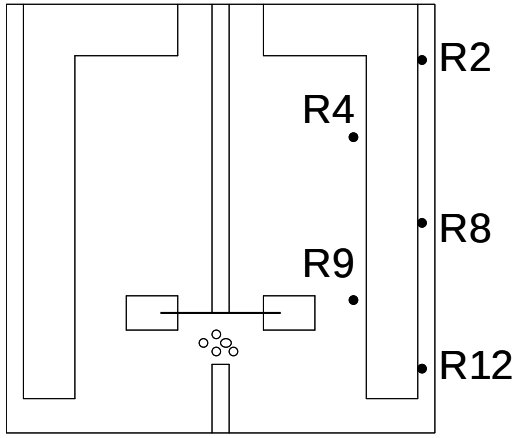

Results – Bubble size distribution

Reactor configuration 1

N **= 157 RPM; 0.052 vvm**

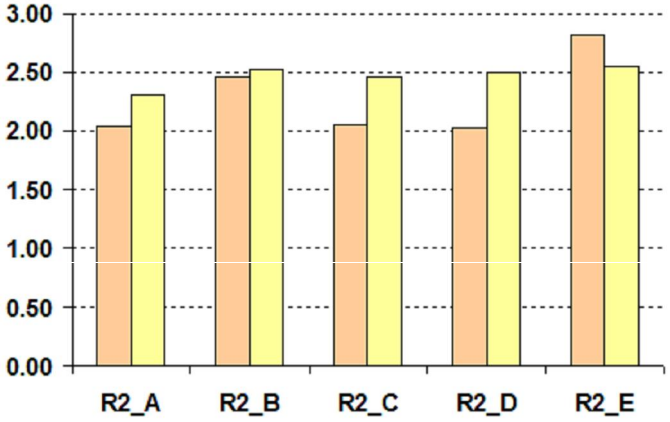

N **= 250 RPM; 0.052 vvm**

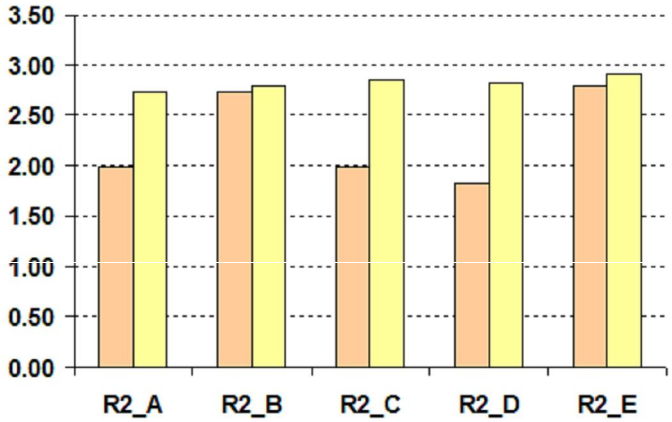

N **= 250 RPM; 0.072 vvm**

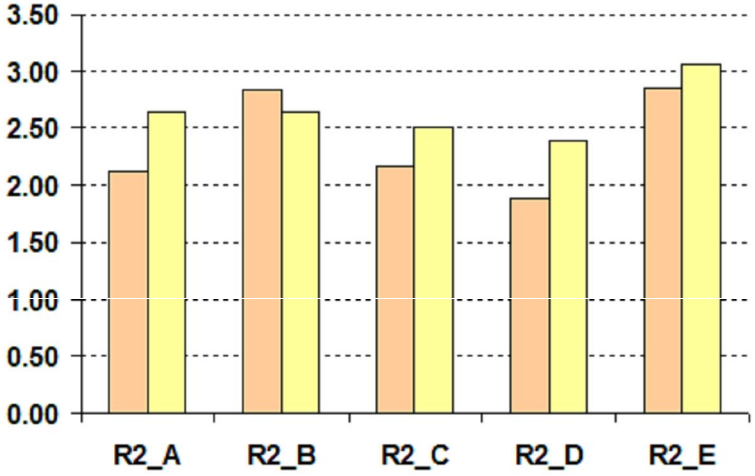

Experimental

Simulation

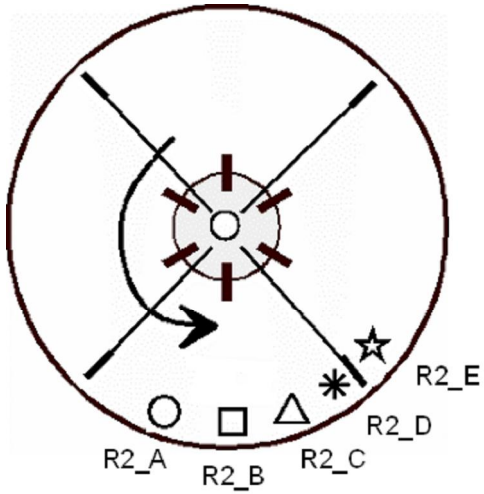

Results – Bubble size distribution

Reactor configuration 2 – *N* = 390 RPM; 0.7 vvm

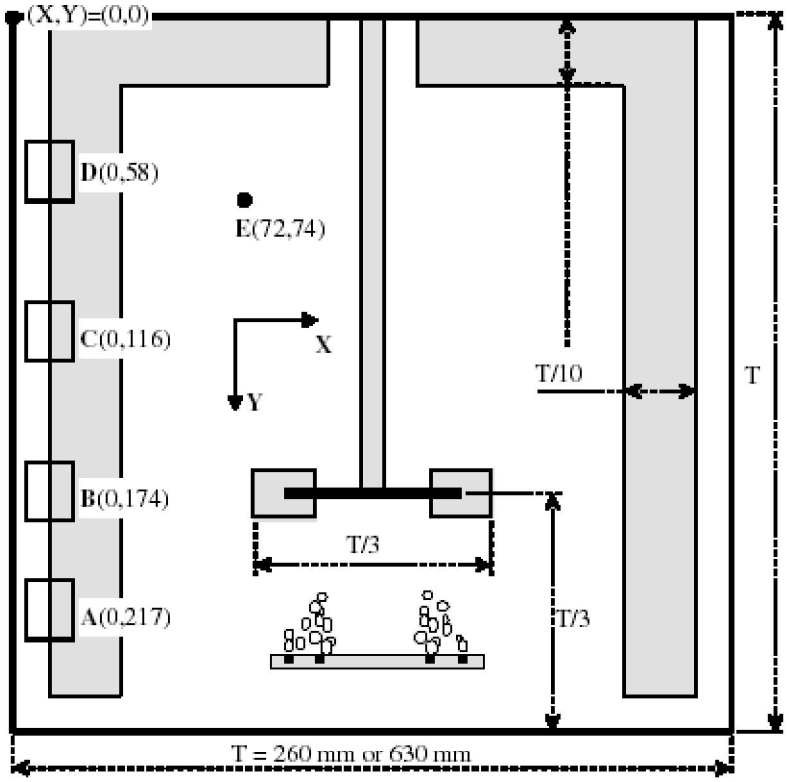

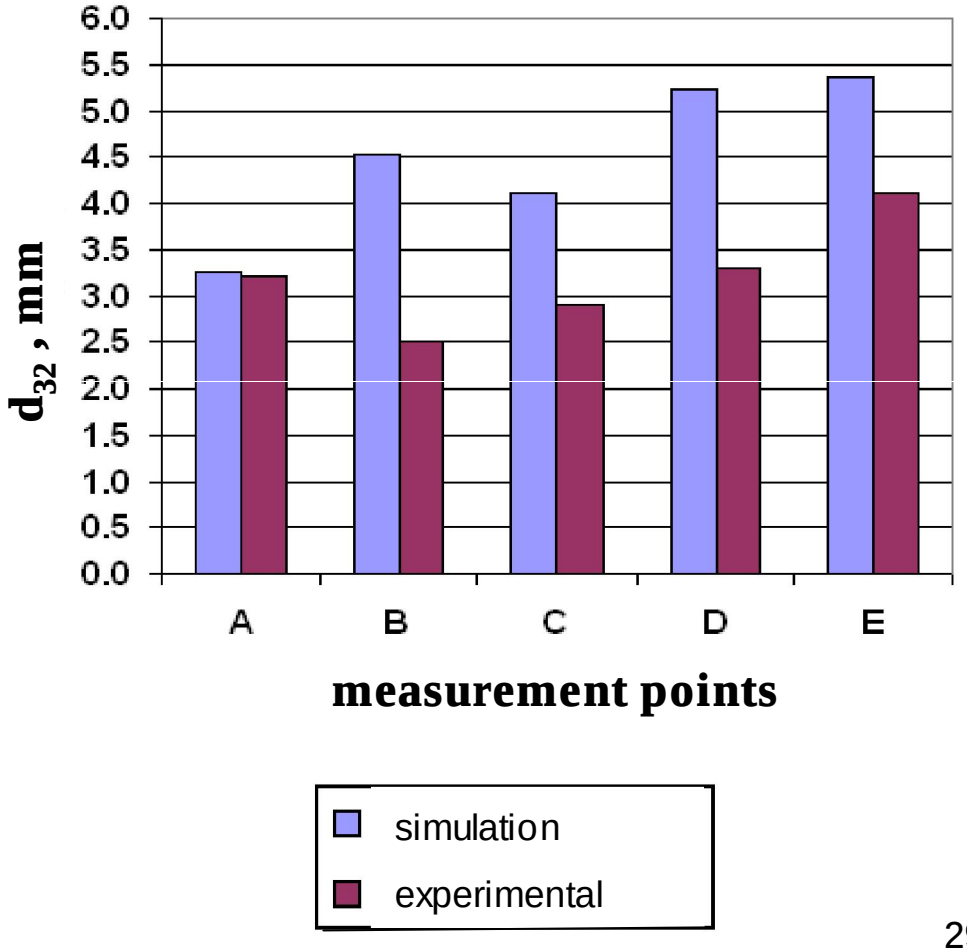

Results – Bubble size distribution

Reactor configuration 2 – *N* = 390 RPM

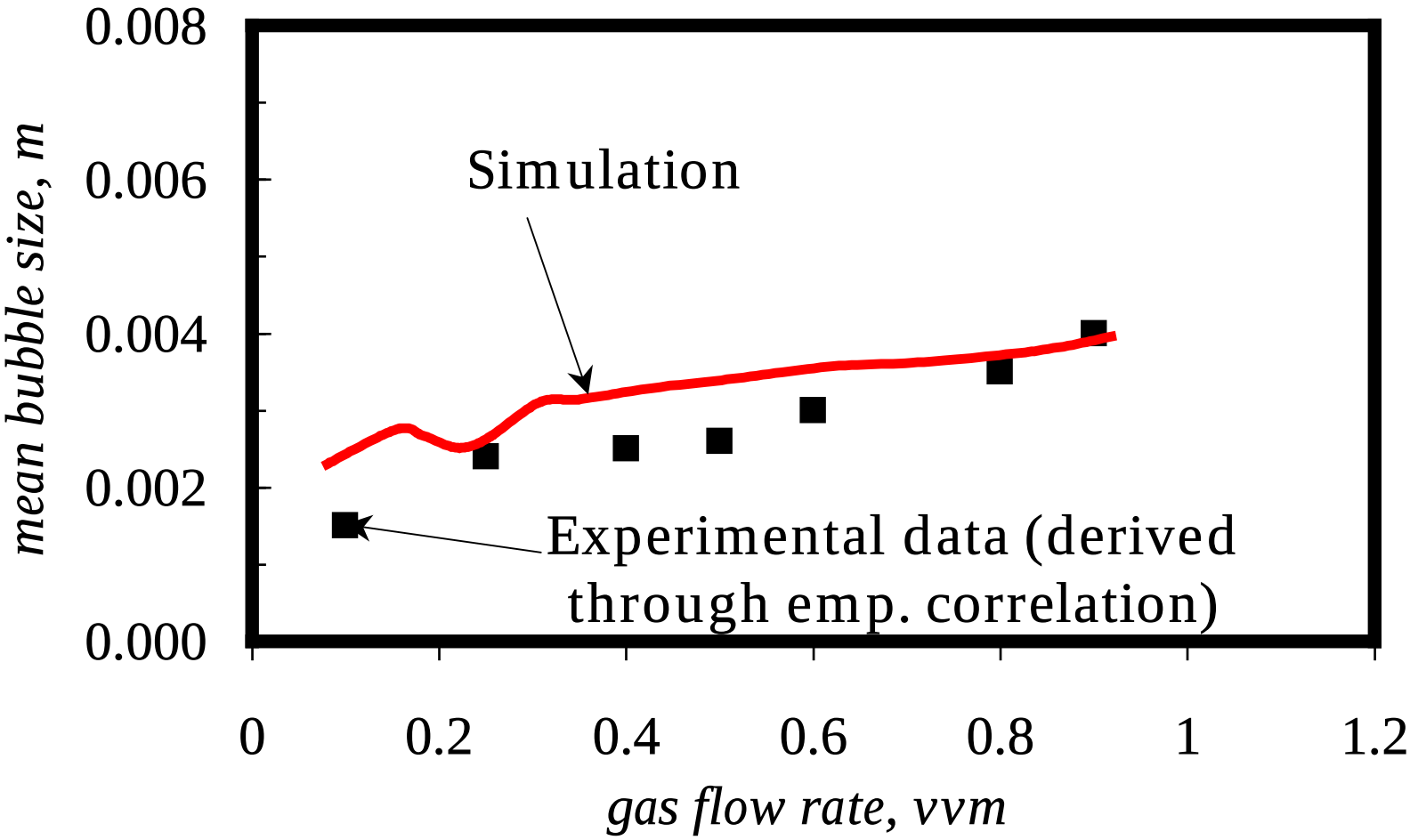

Conclusions

- Some solid **guidelines** for the simulation of gas-liquid stirrer tanks in realistic conditions have been identified and validated.

- **Great attention must be paid to the calculation of the drag force** (this can be calculated via the bubble terminal velocity taking into account the effect of turbulence and of the other bubbles for very high hold-ups)

- The algorithm for the calculation of the bubble size distribution **(QMOM + correction algorithm)** was found to be **stable** under very different operating conditions and reactor configurations.

- The **coalescence and breakage kernels** and the **drag law** are able to describe **with satisfactory accuracy** both the global hold up, the bubble size distribution and the mean bubble size.

- The **simulation settings** can be used to describe the behavior of the stirrer tank under different operating conditions ranging from very **low gas hold-up (0.5 %)** **to** **high gas hold-up** (7 % for the air-water system)

Possible next steps

- Application to mass transfer in gas-liquid systems

Mass transfer in gas-liquid systems is very sensitive to the bubble size distribution, because of the effect of interfacial area and because the transfer coefficient depends on gas-liquid slip velocity (which in turn depends on bubble size). An important point is that there may be a difference between the size range of bubbles that control fluid dynamics (usually the larger ones) and those that determine interfacial area (the smaller ones). This point could be captured well by proper use of the population balance method.

- Gas-liquid chemical reactions

Introduction of chemical reaction paths and interfacial mass transfer models for process reactions in multicomponent two-phase systems. Probable need to consider heat generation/transfer effects as well.

Thank you very much for your kind attention